Appl. Phys. A 87, 27–31 (2007)
DOI: 10.1007/s00339-006-3860-1
Applied Physics A
Materials Science & Processing

Rapid communication

S. SINGH
S.B. KRUPANIDHI✉

Synthesis and structural characterization of the antiferroelectric lead zirconate nanotubes by pulsed laser deposition

Materials Research Centre, Indian Institute of Science, Bangalore 560012, India

Received: 6 October 2006/Accepted: 11 October 2006
Published online: 23 January 2007 • © Springer-Verlag 2007

ABSTRACT For the first time, a pulsed laser ablation deposition (PLD) method has been employed for the synthesis of antiferroelectric lead zirconate, $PbZrO_3$, (PZ) nanotubes within the pores of anodic aluminum oxide (AAO) templates. The structure and morphology of fabricated PZ nanotubes were characterized by number of techniques, including scanning electron microscope (SEM), X-ray diffraction (XRD) and transmission electron microscope (TEM)analysis. After postannealing at 650 °C, the PZ nanotubes exhibited a polycrystalline microstructure, and X-ray diffraction studies revealed that they are of an orthorhombic distorted perovskite crystal structure. TEM analysis confirmed that the obtained PZ nanotubes are composed of nanoparticles in the range of 3–7 nm and the thickness of the wall of the nanotubes is around 10 nm.

PACS 61.46.Fg; 68.37.Lp; 68.37.Hk; 77.80.-e; 81.15.Fg

1 Introduction

Soon after the discovery of carbon nanotubes [1], many groups world-wide became involved in the development of nanotubes of various materials. Nanotube materials are of great interest due to their unusual and different properties compared to their bulk counterparts resulting from their larger surface area, and their relevant applications in mesoscopic physics and nanoscale device fabrication [2–4]. Recently, efforts have been made to synthesize and understand the growth of nanostructures of functionalized materials such as complex ferroelectric oxides because of their promising applications in nanoscale piezoelectric actuators and transducers, nonvolatile memory devices, and ultrasonic devices [5–9]. In developing practical nanoscale devices, an important challenge is the ability to reveal the formation mechanisms of the nanostructures and to rationally exploit their size-dependent properties. As ferroelectricity represents a cooperative phenomenon that relies on the interaction of neighboring permanent electric dipoles in a crystal lattice, there is a size limit, known as the superparaelectric limit, below which ferroelectricity vanishes [10]. Therefore, the synthesis of ferroelectric and antiferroelectric nanostructures of a controllable size and shape is of great interest for future devices applications. Nanotubes of various materials have been synthesized through various methods, among which template based technology provides a versatile technique for synthesizing highly ordered one-dimensional nanostructure materials. The advantages of synthesis of nanostructures through template are (i) the structure of the nanoarray is controlled by the structure of the template, and the material of interest which is inside the pores is confined by the channels of the template, (ii) the aggregation of the guest, which is the material of interest, is blocked by the pore walls of template; and (iii) a large amount of nanowires or nanotubes with the same structure and properties can be synthesized. In addition, it is very useful for large-scale preparation of one-dimensional nanostructures, which is the basic building block of nanodevices. Using the sol–gel template approach of synthesis, Hernandez et. al. have fabricated barium titanate (BT) and lead titanate (PT) nanotubes within 200 nm alumina templates [11]. Recently, Zhang et al. have fabricated highly ordered lead zirconate titanate (PZT) nanowires using sol–gel synthesis within hexagonal closely packed nanochannel alumina templates. They have shown that these highly ordered ferroelectric one-dimensional PZT arrays exhibit a significant piezoresponse and show promise for potential applications [12]. In this manuscript, we are reporting the synthesis of antiferroelectric lead zirconate nanotubes (PZNTs) by means of PLD utilizing porous AAO template. PZ is the most potential antiferroelectric material for sensor and actuator applications in microelectromechanical systems (MEMS) through combination with silicon micromachining technology with which the actuator devices, including micropositioners, micromotors, microvalves, and micropumps, can be widely used in compact medical, automotive, optical, and space systems [13, 14]. PZ has an orthorhombic distorted perovskite structure at room temperature ($a = 0.8231$ nm, $b = 1.1768$ nm, and $c = 0.5881$ nm, JCPDS, #350739) with the crystallographic unit cell containing eight formula units.

✉ Fax: +91 802 3607316, E-mail: sbk@mrc.iisc.ernet.in

2 Experimental

Commercially available anodic aluminum oxide membranes (Whatman®, pore diameter range 190–240 nm, and 60 μm thickness) were used as the templates. Templates were cleaned for 15 min in an ultrasonic bath using solvents of different polarity (distilled water, ethanol, acetone, and hexane). Prior to use, the templates were annealed at 250 °C for 1 h in vacuum to remove any possible impurities. A dense ceramic PZ target was prepared via a conventional solid-state route by ball milling, calcining the multi-component oxides of ZrO_2 (purity 99.99%, Aldrich,) PbO (99.99%, Aldrich) powders at 900 °C for 6 h. The powder was then pressed into circular ceramic pellet of 12 mm diameter and of 4 mm thick and then sintered at 1200 °C for 8 h. Thus a prepared phase well sintered pure PZ target to 97% of the theoretical density was used as the target for PLD for the synthesis of PZNTs. The PLD apparatus and the experimental methods have both been described elsewhere [15]. The PLD chamber was evacuated to a base pressure of 1.2×10^{-6} Torr. The output of a KrF excimer laser (Lambda-Physik COMPex, 248 nm) operating at a pulse repetition rate of 5 Hz was focused onto a rotating PZ target. A laser fluence of $\sim 2.5\ \mathrm{J\,cm^{-2}}$ was employed for ablation and the template was located at 3.8 cm from the target, with its face perpendicular to the target surface normal for the depositions. The deposition was carried out at 400 °C in an oxygen ambience of 50 mTorr. The material filled template was subsequently heated in air at 650 °C for 1 h by using a thermal annealing furnace to obtain the perovskite phase. PZNTs were isolated on removal of the templates by immersing them in 6 M NaOH solution at room temperature for 15 h. To retrieve reasonable quantities of nanotubes, the base solution was diluted in several steps with distilled water and finally with ethanol. When a high power laser beam strikes the PZ target, the target material evaporates and goes inside the pores of the template in the form of a plume which also deposits over the surface of the template. This surface material interconnects the pores over the surface of the template and has to be removed. Such surface films were removed very carefully by mechanically polishing after the heat treatment. The isolated nanotubes were collected by centrifugation. The crystal structure of the PZNTs was investigated using X-ray diffraction (XRD) using a Philips PW3710 diffractometer (Cu K_α radiation, 30 kV and 20 mA, $\lambda = 1.5406$ nm). The morphology of the PZNTs was studied by scanning electron microscopes (SEM) (Sirion 200 and Quanta 200). For SEM analysis, a thin layer of gold was sputtered on the surface of the samples to reduce charging effects. The microstructure was examined by TEM, (Tecnai F30).

3 Results and discussion

The morphology of the PZNTs inside the pores of the alumina template was studied by SEM. Figure 1a shows the etched (with 6 M NaOH solution) regions of the AAO template after the deposition, heat treatment and the mechanical polishing. The micrograph clearly shows the contraction of the nanotubes from the original dimension of the pores. A clear demarcation between the walls of the nanotubes and the walls of the pores can be observed in the Fig. 1a. This also confirms that the template materials do not chemically react with the PZNTs. The reduction in the diameter of the nanotube from the diameter of the pores is attributed to the shrinkage experienced by the PZNTs due to densification involved on heat treatments. Figure 1c shows the energy dispersive X-ray (EDX) spectrum of the PZNTs collected from the solution, which are shown in of Fig. 1b. It is clear from EDX spectrum and data that these nanotubes are composed of equal quantities of Pb and Zr atoms. The emission lines of Al, the etching NaOH solution, reagent, and template were not observed in the spectrum, thereby confirming the absence of alumina from the template and other impurities from the etching solution. The crystallinity and phase purity of the PZNTs were examined by XRD. Figure 2 shows the XRD pattern of the template free PZNTs, which were collected and gathered after several distillations of the NaOH solution. The XRD pattern of the PZNTs clearly shows that the nanotubes are phase pure and no impurity phase was detected. The observed XRD pattern of the PZNTs matches well with the available data (JCPDS, #350739) for the bulk PZ. The orientations and the intensity ratios of the PZNTs matched well with the orthorhombic distorted perovskite phase of bulk PZ.

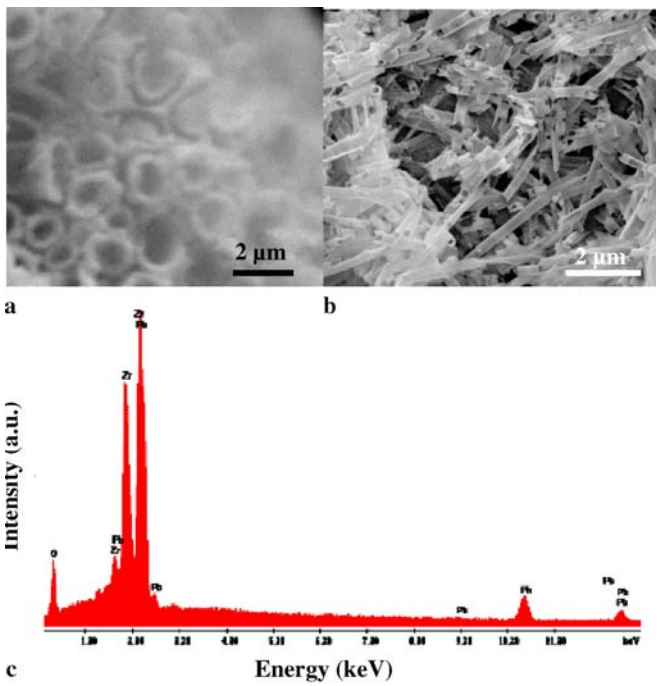

FIGURE 1 SEM images: (**a**) partially etched heat-treated AAO template filled with PZNTs, (**b**) and (**c**) PZNTs after complete removal of AAO template and corresponding EDX spectrum

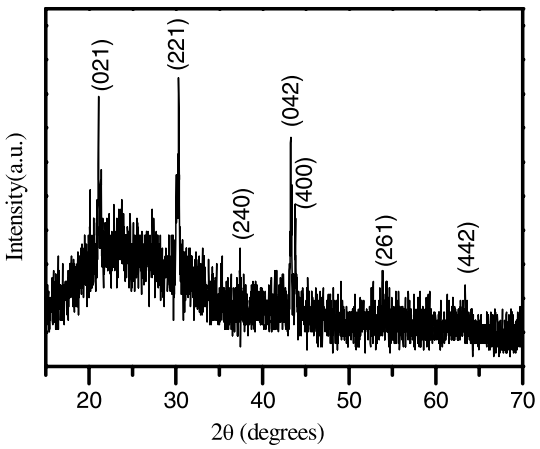

FIGURE 2 XRD pattern of PZNTs

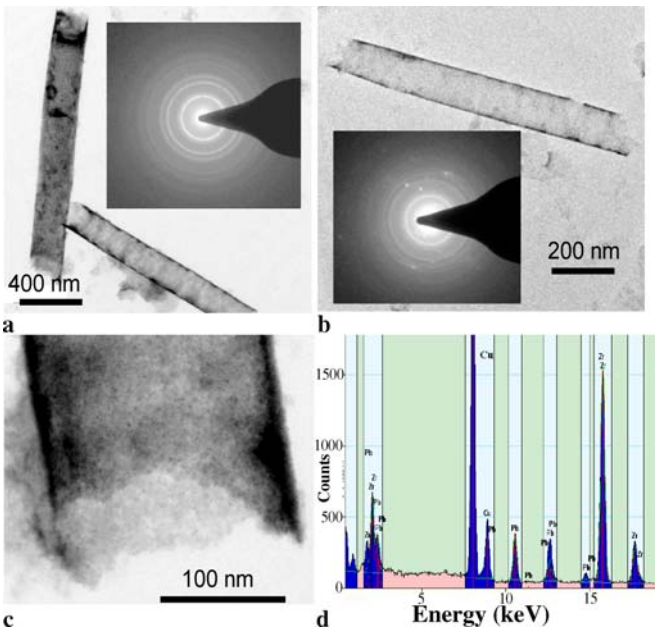

FIGURE 3 TEM images: (**a**) and (**b**) isolated PZNTs and *inset* shows the corresponding SAED, (**c**) end of a nanotube and (**d**) the corresponding EDX pattern

Figure 3a and b shows the TEM images of the isolated PZNTs and the inset shows the corresponding selected area electron diffraction (SAED) patterns. It is apparent from Fig. 3a that the PZ nanostructures synthesized were hollow nanotubes with a distribution with a diameter of around 185–235 nm. The distribution of the diameter of the nanotubes depends mainly on the pore dimensions in the template and they mimic the distributions of the pore dimensions. SAED patterns of these PZNTs shows circular ring pattern, which is common for any polycrystalline structure and the rings correspond to the (221), (240), (042), (261) and (442) planes of the orthorhombic structure of the PZ. The strong intensity ring (221) indicates that the particles are more aligned along the [221] direction. The lattice spacings were calculated from the diameter of the bright circular rings observed in the electron diffraction pattern and compared with XRD data and the data available in the literature. The lattice spacings d_{221}, d_{240}, d_{042}, d_{261} and d_{442} were 2.958, 2.398, 2.077, 1.713 and 1.459 Å respectively, which are in good agreement in the literature. Figure 3c shows the TEM image of the tip of a nanotube. It clearly shows that the average thickness of the wall is around 10 nm. Figure 3d shows the EDX pattern taken by the TEM on a PZ nanotube. From this pattern it is further clear that these nanotubes comprise Pb and Zr and with no other impurities present. The presence of Cu peaks are due to the Cu grids used in TEM analysis.

The high-resolution transmission electron microscope (HRTEM) image taken on the wall of a single PZ nanotube is shown in Fig. 4, which gives further insight into the details of the structure. This HRTEM image clearly shows that the wall consists of a number of nanoparticles, which are randomly aligned in the wall. The distance between the parallel fringes is about 2.985 Å, corresponding to the well-recognized lattice spacing of {211} atomic planes, which agrees well with the values, calculated from the XRD and SAED patterns. This confirms that the walls consist of nanoparticles with preferred (221) orientations. The nanoparticles making up the wall of the nanotubes in other oxide materials, have been observed by various research works and reported elsewhere [16–18]. The size of nanoparticles in the walls were found to be in the range of 3–7 nm, which is also in good agreement with reported data of these functional complex oxide nanostructures [18].

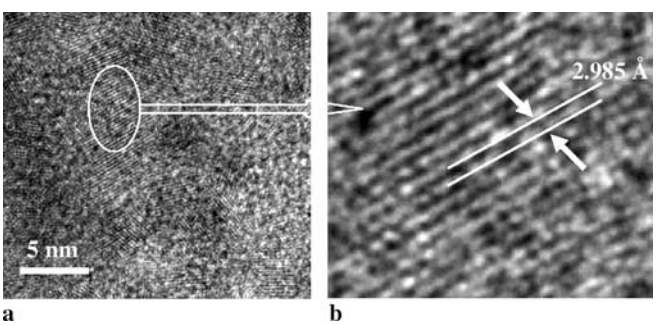

FIGURE 4 (**a**) HRTEM image of a PZNT and (**b**) some magnified region of Fig. 4a

4 Conclusions

In conclusion, PZNTs with diameters of about 185–235 nm were

fabricated for the first time by means of PLD utilizing the closely packed porous nanochannel alumina templates. The crystallinity of the PZNTs were confirmed by XRD and SEAD patterns. Compositional homogeneity and their crystalline structure confirms the formation of orthorhombic distorted perovskite PZNTs. The walls of the nanotubes were found to be made of nanoparticles which was confirmed from the HRTEM image. The average thickness of the well of the nanotubes was found around 10 nm and nanoparticles comprising the wall were found to be in the range of 3–7 nm. These PZNTs may be used in charge pumping devices for various MEMS devices applications.

REFERENCES

1 S. Iijima, Nature **354**, 56 (1991)
2 Y. Xia, P. Yang, Y. Sun, Y. Wu, B. Mayers, B. Gates, Y. Yin, F. Kim, H. Yan, Adv. Mater. **15**, 353 (2003)
3 G.R. Patzke, F. Krumeich, R. Nesper, Angew. Chem. Int. Edit. **41**, 2446 (2002)
4 C.N.R. Rao, M. Nath, Dalton Trans. 1 (2003)
5 J. Junquera, P. Ghosez, Nature **422**, 6931 (2003)
6 Y. Wang, J.J. Santiago-Aviles, Nanotechnology **15**, 32 (2004)
7 Y. Luo, I. Szafraniak, N.D. Zakharov, V. Nagarajan, M. Steinhart, R.B. Wehrspohn, J.H. Wendorff, R. Ramesh, M. Alexe, Appl. Phys. Lett. **83**, 440 (2003)
8 M.W. Chu, I. Szafraniak, R. Scholz, C. Harnagea, D. Hesse, M. Alexe, U. Gosele, Nat. Mater. **3**, 87 (2004)
9 A. Roelofs, I. Schneller, K. Szot, R. Waser, Appl. Phys. Lett. **81**, 5231 (2002)
10 X.Y. Zhang, X. Zhao, C.W. Lai, J. Wang, X.G. Tang, J.Y. Dai, Appl. Phys. Lett. **85**, 4190 (2004)
11 B.A. Hernandez, K.S. Chang, E.R. Fisher, P.K. Dorhout, Chem. Mater. **14**, 480 (2002)
12 X.Y. Zhang, X. Zhao, C.W. Lai, J. Wang, X.G. Tang, J.Y. Dai, Appl. Phys. Lett. **85**, 4190 (2004)
13 D.L. Polla, L.F. Francis, MRS Bull. **21**, 59 (1996)
14 L.E. Cross, S. Trolier-McKinstry, Encycl. Appl. Phys. **21**, 429 (1997)
15 D.B. Chrisey, G.K. Hubler, *Pulsed Laser Deposition of Thin Films* (Wiley, New York, 1994)
16 M. Bognitzki, H. Haoqing, M. Ishaque, T. Frese, M. Hellwig, C. Schwarte, A. Schaper, J.H. Wendorff, A. Greiner, Adv. Mater. **12**, 637 (2000)
17 X.Y. Zhang, C.W. Lai, X. Zhao, D.Y. Wang, J.Y. Dai, Appl. Phys. Lett. **85**, 143 102 (2005)
18 M.C. Hsu, I.C. Leu, Y.M. Sun, M.H. Hon, J. Solid State Chem. **179**, 1421 (2006)